Published in final edited form as:
Cryst Growth Des. 2010 November 15; 10(12): 5007–5019. doi:10.1021/cg1011633.

Nucleation

Peter G. Vekilov
Department of Chemical and Biomolecular Engineering and Department of Chemistry, University of Houston, Houston Texas, 77204-4004, USA

Abstract

Crystallization starts with nucleation and control of nucleation is crucial for the control of the number, size, perfection, polymorphism and other characteristics of crystalline materials. This is particularly true for crystallization in solution, which is an essential part of processes in the chemical and pharmaceutical industries and a major step in physiological and pathological phenomena. There have been significant recent advances in the understanding of the mechanism of nucleation of crystals in solution. The foremost of these are the two-step mechanism of nucleation and the notion of the solution–crystal spinodal. According to the two-step mechanism, the crystalline nucleus appears inside pre-existing metastable clusters of size several hundred nanometers, which consist of dense liquid and are suspended in the solution. While initially proposed for protein crystals, the applicability of this mechanism has been demonstrated for small molecule organic materials, colloids, polymers, and biominerals. This mechanism helps to explain several long-standing puzzles of crystal nucleation in solution: nucleation rates which are many orders of magnitude lower than theoretical predictions, the significance of the dense protein liquid, and others. At high supersaturations typical of most crystallizing systems, the generation of crystal embryos occurs in the spinodal regime, where the nucleation barrier is negligible. The solution-crystal spinodal helps to understand the role of heterogeneous substrates in nucleation and the selection of crystalline polymorphs. Importantly, these ideas provide powerful tools for control of the nucleation process by varying the solution thermodynamic parameters.

Introduction

Due to its crucial place at the start of the crystallization process, the nucleation of crystals determines many properties of the emerging crystalline phase. It is obvious that the nucleation selects the polymorphic form and if a different polymorph is desired, conditions at which its nucleation is faster than that of the other possible polymorphs should be sought. If nucleation is fast, many crystals form nearly simultaneously. Their growth depletes the medium of solute and may lead to cessation of nucleation at the later stages of crystallization. Thus, the majority of crystals grow to approximately identical sizes. In contrast, if nucleation is slow and fewer crystals nucleate at a time, the supersaturation in the solution drops slowly, the nucleation of new crystals continues and a population of crystals of various sizes forms. Ultimately, if nucleation is hindered everywhere in the growth container but at a few selected spots, crystals only nucleate at these spots and grow large before the solution is depleted of nutrient. Hence, control of nucleation is a means to control size, size distribution, polymorphism and other properties of the crystals, Fig. 1.

Here, we review recent advances in the understanding of nucleation of crystals from solution; while important materials are synthesized by the growth of crystals or epitaxial layers form melts or vapor phases, *de novo* nucleation of crystals from the latter two media is seldom carried out and is not extensively studied. Solution crystallization underlies a broad range of industrial, laboratory, and physiological processes. Single solution-grown crystals of inorganic salts or mixed organic-inorganic materials are used in non-linear optics

elements [1] and for other electronic and optical-electronic applications; chemical products and production intermediates are precipitated as crystals in thousands-of-tons amounts. Another area which relies on solution-grown crystals is pharmacy: the slow crystal dissolution rate is used to achieve sustained release of medications: small-molecules organic [2], or protein such as insulin, interferon-α or the human growth hormone [2–6]. If the administered dose consists of a few equidimensional crystallites, steady medication release rates can be maintained for longer periods than for doses comprised of many smaller crystallites. The formation of protein crystals and crystal-like ordered aggregates underlies several human pathological conditions. An example is the crystallization of hemoglobin C and the polymerization of hemoglobin S that cause, respectively, the CC and sickle cell diseases [7–10]. The formation of crystals in the eye lens underlies the pathology of several forms of cataract 11¯12. A unique example of benign protein crystallization in humans and other mammals is the formation of rhombohedral crystals of insulin in the islets of Langerhans in the pancreas 13. Traditionally, protein crystals have been used for the determination of the atomic structure of protein molecules by x-ray crystallography [14]; this method contributes ~ 87 % of all protein structures solved, with the majority of the other determinations carried out by Nuclear Magnetic Resonance (NMR) spectroscopy [15].

Below, we first discuss the thermodynamic and kinetic aspects of the classical nucleation theory, which still represents the main framework for the understanding of nucleation phenomena. Then we consider recent data on the rates of nucleation of protein crystals and show that several of the features of the experimentally determined kinetic dependencies do not comply with the predictions of the classical theory. We then discuss the two-step mechanism of nucleation, according to which the crystalline nuclei appear inside metastable clusters of size several hundred nanometers, which consist of dense liquid and are suspended in the solution. We review recent evidence suggesting that while this mechanism was first proposed for the nucleation of protein crystals, it applies to the nucleation of small-molecule organic and inorganic, as well as colloid and biomineral crystals. We also show that at the high supersaturations employed in many crystallizing systems the nucleation barrier becomes negligible, i.e., the generation of the crystals proceeds in the spinodal regime. We discuss the implication of these findings for the nucleation rate, for the nucleation's response to the presence of foreign surfaces, and for the selection of the polymorph form of the crystallizing material.

The classical nucleation theory

Thermodynamics

The formation of crystals is a first-order phase transition. Accordingly, it is characterized with non-zero latent heat, the crystallization enthalpy ΔH^o_{cryst}. More significant for the kinetics of nucleation is the second feature of first order phase transitions: the discontinuity of the concentration at the phase boundary. As a result of this discontinuity, the solution-crystal boundary possesses non-zero surface free energy. If a small piece of a condensed phase forms in a supersaturated solution, the surface free energy of the emerging phase boundary makes this process unfavorable. Thus, a very limited number of embryos of the condensed phase appear as a result of the few fluctuations which overcome the free energy barrier. The first step in the formation of a new phase, in which the kinetics of the phase transformation is determined by this barrier, is called nucleation.

The thermodynamic part of the classical nucleation theory was developed by J.W Gibbs in two papers [16–17]. We present it here with two modifications: we consider the formation of a crystal in contrast to the J.W Gibbs's consideration of a liquid droplet, and we assume that the initial crystallite is shaped like a cube with a side *a* instead of assuming a spherical droplet of radius *r*. In a supersaturated solution, i.e., one in which the solute chemical

potential is higher than that of molecules in the crystal so that $\Delta\mu = \mu_{solute} - \mu_{crystal} > 0$, the formation of such a cluster leads to a free energy loss of $-n\Delta\mu$. On the other hand, the creation of the phase boundary with area S and surface free energy α between the cluster and the solution leads to a free energy gain $S\alpha$. Assuming that the crystal cluster is a cube, $S = 6a^2n^{2/3}$; other shapes will lead to coefficients different than $6a^2$ in this relation, but the 2/3 scaling with n will be preserved for all three dimensional nuclei. Thus,

$$\Delta G(n) = -n\Delta\mu + 6a^2n^{2/3}\alpha. \quad (1.)$$

This dependence is plotted in Fig. 2.

Differentiating $\Delta G(n)$, we find the cluster size n^* for which ΔG passes through a maximum ΔG^*

$$n^* = \frac{64\Omega^2\alpha^3}{\Delta\mu^3} \text{ and } \Delta G^* = \frac{32\Omega^2\alpha^3}{\Delta\mu^2} = \frac{1}{2}n^*\Delta\mu, \quad (2.)$$

where $\Omega = a^3$ is the volume occupied by a molecule in the crystal.

As Fig. 2 illustrates, ΔG^* is the barrier that must be overcome to form a crystal from solute molecules. The growth of clusters smaller than n^* is associated with an increase of free energy and is unfavorable. Clusters may still grow to such sizes as a result of a fluctuation, but since a driving force exists for the decay of these clusters, such events are rare. On the other hand, if as a result of a fluctuation a cluster reaches as size greater than n^*, its growth is accompanied by a decrease of free energy and occurs spontaneously. A cluster of size n^* has equal probabilities of growth and decay and, hence, such clusters are called critical and they represent the nuclei of the new phase. Note that by this definition all nuclei are critical and the term “critical nuclei” is redundant [18].

The rate of crystal nucleation

To model the nucleation rate J, i.e., the number of nuclei which appear is a unit solution volume per unit time, M. Volmer postulated—in analogy to the Arrhenius equation—that $J = J_0\exp(-\Delta G^*/k_BT)$, where k_B is the Boltzmann constant [19]. The external parameters, such as temperature, concentration and pressure, as well the solution supersaturation, affect the nucleation rate mostly through ΔG^* according to Eq. (2); the effects on J_0 are significantly weaker. There are numerous statistical-mechanical derivations of the nucleation rate law within the assumption of the classical nucleation theory, for an example, see Ref. [20]. The final expression of these derivations can be represented as [21]

$$J = \nu^* Zn \exp(-G^*/k_BT). \quad (3.)$$

where ν^* is the rate of attachment of monomers to the nucleus, Z is the Zeldovich factor, which accounts for the width of the free energy profile $\Delta G(n)$ in the vicinity of the maximum ΔG^*, see Fig. 2, and n is the number density of molecules in the solution. Eq. (3) assumes that the replacement partition function of the nucleus [20–21] is equal to one. This factor accounts for the additional stabilization of the nuclei due to their translational and rotational degrees of freedom [22]. Neglecting it is a reasonable assumption for crystal nuclei suspended in a viscous solution; this would not be the case for nucleation in the gas phase.

A major assumption in the derivation of Eq. (3) is that the solute molecules exchange directly with the crystalline embryo. To understand the meaning of this assumption and why it might not apply to nucleation of crystals in solution, we need to step back and consider the distinction between a solution and a crystal.

Let us start with the phase diagram of a solution in coordinates concentration and temperature at constant pressure. This phase diagram typically contains three equilibrium phases: a dilute solution, a dense liquid, and crystal; a higher number of phases are possible if more than one crystalline polymorph may form; kinetically arrested states, such as gels, are sometimes included in the phase diagram. While with some solutions of small-molecule compounds the dense liquid might not be observable, the dense liquid is readily seen in protein, colloid, and some organic solutions 23–26. To distinguish between the three phases present in the phase diagram, at least two parameters, called order parameters, are needed. Thus, the dilute solution and the dense liquid differ by the solute concentration, the dense liquid and the crystal differ by structure (there may be a slight difference in concentration), and the dilute solution and the crystal differ by both concentration and structure.

From this point of view, the formation of crystals in solution should be viewed as a transition along two order parameters: concentration and structure[18]. While a transition along the concentration axis is easy to imagine, structure transitions appear less trivial. Pure structure transitions are only possible in melts, whose concentration is similar to that of the emerging crystalline phase. Crystalline nuclei form as a result of a fluctuation along the structure axis. The smallest structure fluctuation can be viewed as a pair of molecules from the melt that has an orientation identical to the orientation of a pair of molecules in the crystal, for informative examples, see Refs [62,63]. This crystal-like orientation in the pair is preserved over times significantly longer than the lifetime of a “bond” in the melt. A nucleus arises as a result of accumulation of such ordered pairs into an ordered piece of new phase. In a sense, structure fluctuations can be viewed as fluctuations of the density of ordered pairs.

If a crystal nucleates not from its melt, but from a dilute solution or gas, both a concentration and a structure fluctuation are needed so that a crystalline nucleus may form, Fig. 3a. Thus, the above assumption that an ordered nucleus forms directly in the dilute solution corresponds to the assumption that the solution to crystal transformation occurs as a transition along both order parameters, density and crystallinity, simultaneously; in Fig. 3a this pathway is represented by the arrow along the diagonal of the (Concentrations, Structure) plane. It could be argued that a more energetically favorable pathway is for the transition is to proceed along the two order parameters in sequence. Such a sequential pathway would correspond to the formation of droplet of a dense liquid followed by the formation of a crystalline nucleus inside this droplet, as illustrated in Fig. 3b.

This mechanism was first suggested by simulations and analytical theory 27–29. These theoretical efforts predicted that the density and structure fluctuations are only separated near the critical point for liquid-liquid (L-L) separation occurring in model protein solution systems[27], 30–31, while for off-critical compositions, the fluctuations of the density and structure order parameters occur synchronously27, similarly to the classical viewpoint.

The experiments discussed below demonstrate that nucleation of crystals of the protein lysozyme, under a broad range of conditions, proceeds in two steps: the formation of a droplet of a dense liquid, followed by nucleating a periodic crystal within the droplet [32–35], as schematically illustrated in Fig. 3. If the dense liquid is stable with respect to the dilute solution—this case is represented by the lower curve in Fig. 3c—the nucleation of crystals occurs inside macroscopic droplets of this phase. A far more common case is when the

dense liquid is not stable but has a higher free energy than the dilute solution [24–25], represented by the upper curve in Fig. 3c. In these cases, the dense liquid is contained in metastable clusters, intriguing objects in their own right, and crystal nucleation occurs within the clusters.

After and concurrently with the evidence for the operability of the two-step mechanism in the case of lysozyme crystallization, additional experimental results demonstrated that this mechanism applies to many other proteins, to small molecule organic and inorganic compounds, including biominerals, and colloids. Below, we discuss these and other issues related to the two-step nucleation mechanism

Experimental data on the rate of nucleation of crystals

To understand the mechanism of nucleation of crystals in solution we turn to data on the dependence of the nucleation rate on supersaturation for crystals of the protein lysozyme, a convenient and often used model system. The dependencies of the homogeneous nucleation rate of lysozyme crystals on the thermodynamic supersaturation $\sigma \equiv \Delta\mu/k_BT$, where $\Delta\mu$ is the surplus of the chemical potential of the solute over that of the crystal, at three different concentrations of the precipitant, NaCl, are presented in Fig. 4. The data in Fig. 4 were obtained using the technique for direct determination of the nucleation rates of proteins discussed in Refs. [36–37], which allows distinction between homogenously and heterogeneously nucleated crystals so that the data points in Fig. 4 are homogenous nucleation rates. In support of the conclusion that the rates plotted in Fig. 4 characterize homogeneous nucleation is the fact that they are lower by several orders of magnitude than those stemming from less careful measurements which may have been contaminated by heterogeneous nucleation events [37–40]

Each data series in Fig 4 corresponds to nucleation experiments carried out at a fixed precipitant concentration and at fixed temperature. In agreement with general expectations and Eq. (3), the nucleation rate increases exponentially with supersaturation at each of the three precipitant concentrations, and, overall, is higher at higher precipitant concentrations. However, the dependencies contain four peculiarities.

- **i.** The $J(\sigma)$ dependence at the highest precipitant concentration, C_{NaCl} = 4 %, breaks at $\sigma > 3.1$ and, in dramatic contrast to prediction of Eqs. (2) and (3), the section above this concentration is practically steady as supersaturation increases.
- **ii.** At $\sigma > 3.45$ in the same $J(\sigma)$ dependence, the data scatter increases and three of the recorded points deviate significantly from the dominant trend.
- **iii.** The measured nucleation rates are of order 0.1 – 1 $cm^{-3}s^{-1}$, which is about ten orders of magnitude less than the prediction of the classical nucleation theory; the estimate of J stemming from the classical nucleation theory is discussed below.
- **iv.** The dependence of the nucleation rate on temperature, shown in Fig. 5 presents another puzzling complexity: as supersaturation is increased upon lowering of temperature, the nucleation rate first increases exponentially, as expected from the classical theory, but then passes through as sharp maximum and recedes following a weaker dependence.

In the following subsections, we discuss these four peculiarities.

The nucleus size and solution-crystal spinodal

To understand the breaking *J(C)* dependency, feature (i) above, we use the nucleation theorem to determine the size of the critical nucleus for crystallization. According to Eq. (2),

the number of molecules in the nucleus n^* largely determines the height of the free energy barrier for nucleation ΔG^*, and hence the nucleation rate J. The nucleation theorem [41–44], a universal, model-independent nucleation law, provides an estimate for n^* from the nucleation rate J,

$$n^* - n_0 = k_B T \frac{\partial \ln J}{\partial \Delta \mu} + \alpha_1, \quad (4.)$$

where α_1 is a correction that takes values between 0 and 1 [42].

Figure 4b indicates that at C_{NaCl} = 2.5 and 3 %, n^* does not change throughout the respective supersaturation ranges, while at C_{NaCl} = 4 % the nucleus size changes abruptly at σ = 3.1, corresponding to C = 33.5 mg/ml. The value of the parameter n_0, which roughly corresponds to the number of solute molecules displaced by the nucleus, can be roughly estimated as less than 1. Then the nucleus sizes $n^* - n_0$, extracted from the four linear segments in Fig. 4b are 10, 4, 5 and 1 molecules, respectively. From here we see that the breaking in the $J(C)$ dependence at C_{NaCl} = 4 % is due to the transition of the nucleus size from five to one molecules.

Nucleus size $n^* - n_0 = 1$ means that every molecule in the solution can be an embryo of the crystalline phase, and the growth to dimer and larger clusters occurs with a free energy *gain*. Thus, the free-energy barrier for the formation of the crystalline phase ΔG^* is below the thermal energy of the molecules. In analogy to the nucleation of a fluid within another fluid, we call *spinodal* the phase line at which the nucleation barrier vanishes and the rate of generation of the new phase is only limited by the kinetics of growth of its clusters. The spinodal is defined as the boundary between metastability and instability of an “old” phase, supersaturated with respect to a “new” phase [16–17, 45].

The case discussed here, the solution-solid phase transition, is one for which a mean-field free energy expression encompassing both phases cannot be formulated because of different standard states. Since the inflection point in the dependence of ΔG on the order parameter along which the phase transition occurs is typically used to define the spinodal [46–48], a thermodynamic definition of the solution-crystal spinodal is impossible [46]. The definition proposed here is a kinetic one, based on the transition to nucleus size of *one* molecule, i.e., to where no thermodynamic barriers for the formation of the crystalline phase exist.

In Fig. 6, we have depicted the solution-crystal spinodal line in the (C,T) plane, determined as the concentration C at the transition to $n^* - n_0 = 1$ from Ref. [49]. Since at concentrations and temperature below this spinodal line $\Delta G^* \approx 0$, the nucleation rate J does not increase as supersaturation is increased by increasing C or lowering T. This explains puzzle (i) above. The existence of a solution-crystal spinodal also helps to explains the maxima in the dependencies of the nucleation rate J on temperature in Fig. 4, puzzle (iv) above; for a further details and a theoretical model of these factors, see below.

The transition to a spinodal regime of crystal formation also explains the increased data scatter of $J(\sigma)$ at $\sigma > 3.45$, puzzle (ii) above. As shown in Ref. [34, 50], at the point of transition from nucleation to spinodal decomposition the nucleation rate undergoes a sharp maximum: on the one side is an ascending branch due to the decrease of the size of the nucleus, and on the other side is a descending branch due to the temperature decrease and associated kinetic factors. Near this maximum, the nucleation rate is very sensitive to variations of the experimental conditions: temperature, protein and precipitant concentrations, and others. Hence, minor inconsistencies of these parameters may lead to significant variations in J [33].

The classical theory overestimates the crystal nucleation rate by 10 orders of magnitude

To understand puzzle (iii) above, we use Eq. (3) for an estimate of the crystal nucleation rate based on the classical nucleation theory. The rate ν* can be evaluated form the rate of attachment of molecules to lysozyme crystals at similar protein concentrations. As discussed is Ref. [51], the surfaces of crystal growing in solution are smooth and molecules only attach to growth steps which occupy about $10^{-3} – 10^{-2}$ of the crystal surface. Hence, the rate of attachment to crystals should be estimated from the velocity of step propagation rather than from the rate of growth of the crystal faces.

There are numerous determinations of the step velocities of lysozyme crystals [52–54]. At temperatures and concentrations similar to those during the determination of the nucleation rate in Fig. 4 the step velocities are ~ 1 μm s^{-1}. This yields, with molecular size of lysozyme of 3.5 nm, attachment rate to the steps ~ 300 s^{-1}. In contrast to that of large crystals, the nucleus surface is likely rough (because of the small size of the nucleus) and molecules can attach anywhere. Hence, we assume that ν* ≈ 300 s^{-1}. This estimate of ν* should be viewed as approximate since the configuration of molecules in a kink on the smooth crystal fact during crystal growth may be significantly different than the molecular configuration on the rough surface of a near-critical cluster. Hence, the barriers encountered by an incoming molecule may also differ. On the other hand, estimates of ν* from the diffusion rate of molecules in the solution would yield a significant overestimate since they would completely neglect this barrier, which can be of order several tens of kilojoules per mole [55–56].

The Zeldovich factor Z accounts for the width of the free energy profile along the nucleation reaction coordinate around the location of the maximum [18, 20, 57–58]. It is expected to be of order 0.1 – 0.01 for nucleation of any protein condensed phase [18, 58–59]. The protein number density in a solution of concentration ~50 mg ml^{-1} as the one used for the experiments in Fig.4 [60] is $n = 2 \times 10^{18}$ cm^{-3}. With these values for ν*, Z and n, the pre-exponential factor in Eq. (3) is of order $10^{19} – 10^{20}$ cm^{-3} s^{-1}.

The nucleation barrier ΔG^*, determined from the slope of the dependencies in Fig. 4b, $\Delta G^* \approx 10^{-19}$ J. We can use Eq. (2) to evaluate the surface free energy α of the interface between the dense liquid and the solution from the value of ΔG^*. From the crystal structure, $\Omega \cong 3 \times 10^{-20}$ cm^3 [61]. We get α = 0.5 – 0.6 erg cm^{-2} Ref. [59], which is close to determinations for number of other protein crystals [62–63] and this correspondence supports the estimate of ΔG^* from the data in Fig. 4.

Combining the estimate for the pre-exponential factor with this estimate for ΔG^* we get from Eq. (3) a prediction for $J \approx 10^8 – 10^9$ cm^{-3} s^{-1}. This value is about 10 orders of magnitude higher than those in Fig. 4. It is important to note that since we estimate ΔG^* from experimental data, the difference between the experimentally determined J and the prediction of the classical nucleation theory is due to an overestimate of the pre-exponential factor by the classical theory.

The two-step mechanism of nucleation of crystal in solution

To understand puzzles (iii) and (iv) above, that the nucleation rate is lower by many orders of magnitude than the prediction of the classical theory and the non-monotonic dependence of the nucleation rate on temperature, we show below that the nucleation of crystals occurs inside metastable mesoscopic clusters of dense protein liquid, as illustrated in Fig. 3.

Direct observations of ordered nuclei forming within the dense liquid exist, but only for the case of stable dense protein liquid, Fig. 7 [64–65]. Such direct imaging would be difficult or impossible for the more common case in which the dense liquid is unstable. The action of

the two-step mechanism in this case is inferred from two pieces of evidence: First, we demonstrate the existence metastable mesoscopic dense liquid clusters in solutions. Then, we analyze of the complex kinetic curves in Figs. 4 and 5, propose a kinetic law for the two-step mechanism and show that its predictions qualitatively and quantitatively agree with the experimental data.

Dense liquid clusters in the homogenous region of the phase diagram

If crystallization is carried out at a point in the phase diagram where the dense liquid is unstable, all density fluctuations are expected to decay with a characteristic time of order of the diffusion time of the protein molecules, 10 μs, see below [66–68]. Since the molecules in the region of high concentration within the fluctuation move with the same characteristic time, it would be impossible for them to probe various structures and find the right one for the crystalline nucleus. Thus the crucial question for the understating of nucleation from dilute media is: How does the transition along the order parameter concentration occur? The answer lies in the recently discovered metastable mesoscopic clusters of dense liquid.

The evidence for metastable dense liquid clusters comes from monitoring solutions of three hemoglobin variants, oxy-HbA, oxy-HbS, and deoxy-HbS 66, and the proteins lumazine synthase 68–69 and lysozyme [67], by dynamic light scattering (DLS) and atomic force microscopy [70]. Fig. 8a shows a typical intensity correlation function of a lysozyme solution in the homogeneous regions of the phase diagram. The correlation function reveals two processes: the faster process, with characteristic time τ_1 of order 10 – 100 μs, is the Brownian motion of single lysozyme molecules; it is present at all solution concentrations. The corresponding hydrodynamic radius, determined via the Stokes-Einstein equation, is about 1.5 nm and matches well the diameter of a lysozyme molecule of 3.2 nm. The slower process has a characteristic time τ_2 of order milliseconds; its amplitude increases with higher lysozyme concentrations. This longer time could come from either compact lysozyme clusters suspended in the lysozyme solution, or from single lysozyme molecules embedded in a loose network structure constraining their free diffusion. Since the measured low-shear viscosity of lysozyme solutions is equal to those determined using high shear rates [71], no loose networks in lysozyme molecules exist in these solutions and we conclude that long times in Fig. 8a indeed correspond to lysozyme clusters[66]. The time-dependence of their radius is shown in Fig. 8c and it shows that the clusters appear immediately after solution preparation; their radius is relatively steady. We therefore conclude that these are clusters of dense liquid.

The number density n_2 of the dense liquid clusters and the fraction of the total solution volume ϕ_2 they occupy are evaluated from the amplitudes A_1 and A_2 of the respective peaks in the distribution function [66]. Further results on the behavior of clusters of dense liquid in solutions of hemoglobin and lumazine synthase are presented in Refs.[66, 68–69]. It was found that with all studied proteins, the clusters exist in broad temperature and protein concentration ranges. The clusters occupy ϕ 10^{-6} – 10^{-3} of the solution volume and have number densities of order 10^5 – 10^{10} cm^{-3} Ref. [66].

To evaluate the lifetime of the lysozyme clusters, we note that cluster decay processes contribute a q-independent component to the overall rate $\Gamma_2 = \tau_2^{-1}$ sensed by DLS Ref. [72], $\Gamma_2 = \Gamma_0 + D_2q^2$, and can be distinguished from cluster diffusion. (Γ_0 is the rate of cluster decay, D_2 is the cluster diffusion coefficient, and q is the wave-vector.) The q-dependent, diffusion component indeed dominates the DLS signal, Fig. 8d. Using $\Gamma_0 << D_2q^2$ with q^2 = 3.5×10^{10} cm^{-2} and $D_2 = 2 \times 10^{-9}$ cm^2s^{-1}, $\Gamma_0 \ll 70$ s^{-1}, we obtain a lower bound $1/\Gamma_0 \approx$ 15 ms for cluster lifetimes.

The determination of the lifetime of the clusters of lumazine synthase was more straightforward and yielded an estimated of ~10 s [68–69]. In addition to detection by dynamic light scattering, clusters of lumazine synthase were directly imaged by atomic force microscopy, Fig. 8b [68–69], which confirmed their macroscopic lifetimes and their size.

The lifetimes of the clusters (> 15 ms for Hb and lysozyme and ~ 10 s for lumazine synthase) significantly exceed the equilibration times of the protein concentration at sub-micrometer length scales, i.e. ~10^{-5} s. Thus the compact clusters represent a *metastable* phase separated from the bulk dilute solution by a free energy barrier.

Attempts to rationalize the finite size of clusters have focused on a balance of short-range attraction, due to van der Walls, hydrophobic or other forces, and screened Coulombic repulsion between like-charged species[73–74]. While small clusters which contain about ten particles, naturally appear in such approaches, large clusters are expected only if the constituent particles are highly charged, with about hundreds elementary charges. Such high charges are feasible for micron-size colloidal particles; however, proteins in solution are known to carry less than 10 elementary changes per molecule. Hence, while for colloidal suspensions these theories successfully predict aggregation [75–77], or even the existence of metastable clusters [78], we conclude that a distinct mechanism is at work in protein systems, where clusters contain as many as 10^6 molecules [67]. A recent study concluded that the clusters consist of a non-equilibrium mixture of single protein molecules and long-lived but ultimately unstable complexes of proteins [67]. The puzzling mesoscopic size of the clusters is determined by the lifetime and diffusivity of these complexes. Several possible mechanisms of complex formation: domain swapping, hydration forces, dispersive interactions, and other, system-specific interactions were highlighted.

The rate law for the two-step mechanism of crystal nucleation

A phenomenological theory was developed that takes into account intermediate high-density metastable states in the nucleation process [50]. The rate law for the dependence of the nucleation rate on protein concentration and temperature emerging from this theory is

$$J=\frac{k_2 C_1\, T \exp(-\frac{\Delta G_2^*}{k_B T})}{\eta(C_1,T)\left[1+\frac{U_1}{U_0}\exp(\frac{\Delta G_C^o}{k_B T})\right]}, \tag{5.}$$

where the constant k_2 scales the nucleation rate of crystal inside the clusters, C_1 is the protein concentration inside the clusters, i.e., ~ 300 mg ml^{-1}, ΔG_c^o is the barrier for nucleation of crystals inside the clusters, η is the viscosity inside the clusters, U_1 and U_0 are the effective rates of, respectively, decay and formation of clusters at temperature T, and ΔG_c^o is the standard free energy of a protein molecule inside the clusters in excess to that in the solution, depicted schematically in Fig. 3c [50]. Recent experimental determinations indicate that ΔG_c^o is of order 10 $k_B T$ [67].

Following Ref. [79], the nucleation barrier ΔG_2^* in the vicinity of the solution-crystal spinodal was modeled as

$$\Delta G_2^*(T)=\frac{E^*}{(T_e-T)^2}\left[1-\frac{(T_e-T)^2}{\left(T_e-T_{sp}\right)^2}\right], \tag{6.}$$

where E^* is a parameter, T_e is the temperature, at which a solution of the studied concentration is in equilibrium with a crystal, and T_{sp} is the spinodal temperature. T_e and T_{sp} are determined from the phase diagram in Fig. 6, and E^* is determined by fitting Eq. (7) to the slope of the $J(C)$ dependencies in Fig. 4b.

The viscosity inside the dense liquid clusters was modeled as

$$\eta=\eta_0\{1+[\eta]C_1\exp(k_\eta[\eta]C_1)\}\exp(-E_\eta/k_BT), \quad (7.)$$

where [η] is the viscosity increment, and k_η and E_η are constants; all three viscosity parameters are determined from the known dependencies of viscosity in the studied solution on temperature and concentration.

A crucial assumption is Eq. (7) is that the concentration inside the dense liquid clusters C_1 increases as temperature is lowered, in agreement with the phase diagram in Fig. 6 and the likely similarity between the dense liquid in the clusters and the stable sense liquid depicted in the phase diagram [50]. As a result of this $C_1(T)$ dependence, the viscosity η increases much more strongly in response to decreasing temperature T then suggested by the quasi-Arrhenius member of Eq. (7) with E_η about 10–20 kJ mol^{-1} [80].

The denominator of Eq. (5) offers another pathway by which decreasing temperature affects the nucleation rate J, besides the temperature dependence of the viscosity. Since $(U_0/U_1)\exp(-\Delta G_c^o/k_BT)$ is the non-equilibrium volume fraction occupied by the clusters ϕ_2, the term in the square brackets in the denominator of Eq. (5) is approximately ϕ_2^{-1}. Since $\Delta G_c^o>0$, see above, lower T leads to a greater value of the denominator, which corresponds to a lower volume of the dense liquid clusters and accordingly to lower J. This contributes about factor of five in the decrease in J as temperature is lowered from T_{sp} to the lowest values probed in Fig. 5.

Using Eqs. (5) – (7) nucleation rate data at varying temperature and protein concentrations in Fig. 4 and Ref. [81], as well as non-monotonic dependencies of the nucleation rate on temperature in Fig. 5 were reproduced with high fidelity using literature values or independently determined parameters of the thermodynamic and kinetic parameters of the system [50]. The good correspondence between the model results and the experimental data supports the validity of the two-step nucleation mechanism. According to Eq. (5), the increasing part of the $J(T)$ as temperature is lowered below T_e is due to the increase of the supersaturation Δμ which shrinks ΔG_2^* according to Eq. (2); this leads to exponential increase in the nucleation rate J. The maximum in $J(T)$ is reached exactly at $T = T_{sp}$, where ΔG_2^* vanishes; note that T_{sp} is independently determined from plots similar to the one at 4 % in Fig. 4c [81]. The steep decrease in the nucleation rate as T is lowered beyond the maximum at T_{sp} is a a crucial part in the proof of the validity of the two-step mechanism: within the two-step mechanism this steep decrease is explained by the smaller volume of the dense liquid clusters at lower temperature, and by the higher concentration inside them, leading to higher viscosity. Both the lower volume of the clusters and the higher viscosity lead to lower nucleation rate.

No pathway of steep decrease of nucleation rate beyond the spinodal temperature exists if one assumes one step nucleation: nuclei forming within the dilute solution would be exposed to its viscosity, which is a weak function of temperature. Thus, the nucleation rate would decrease almost imperceptibly, by ~ 16 %, assuming E_η = 20 kJ mol^{-1}, within the 5 – 6 K range probed. Note that the decrease in nucleation rate in glass-forming melts in response to temperature decrease, interpreted as a result of viscosity increase in the melt, occurs over 40

– 50 K [82]; furthermore, this response is significantly enhanced by the stronger temperature dependence of viscosity of melts as compared to that of solutions.

To understand puzzle (iii) above, that the nucleation rate is lower by 10 orders of magnitude than the prediction of the classical theory, we compare the nucleation kinetic law in Eq. (5) to that in Eq. (3). We see that $k_2\phi_2 C_1 T/\eta$ takes the place of the product νZn. In solutions of concentration C in the range 20 to 60 mg ml^{-1} as the ones in which the nucleation rates in Fig. 4 were measured, the cluster volume fraction ϕ_2, represented by the denominator in Eq. (5), is of order 10^{-7}–10^{-6}. With the concentration C_1 in the clusters around 300 mg ml^{-1}, Eq. (7) shows that the viscosity η of the dense liquid in the clusters is around 100 centiPoise, or ~ 100 × higher than in the normal solution. We get that the nucleation rate should be ~ 10^9× lower than the prediction of the classical theory, which assumes nucleation in the solution bulk.

The rate determining step in the two-step nucleation mechanism

The derivation of Eq. (5) is based on the assumption that the first step in the two-step mechanism, the formation of the dense liquid clusters is fast and that the second step, the formation of the crystal nuclei within the dense liquid clusters, is rate determining. While the excellent agreement between the experimental data and the prediction of Eq. (5) in Fig. 5 can be viewed as a support of this assumption, it should and can be tested independently.

As first evidence in favor of the fast rate of generation of the dense liquid clusters, we view data on the time dependence of three characteristics of the cluster population: average radius, number density, and volume fraction, illustrated for the case of average cluster radius in Fig. 8c. All of these dependencies, monitored for the proteins lumazine synthase [68–69], lysozyme [67], and three hemoglobin variants [66] reveal that the clusters appear within several seconds of solution preparation. After that, the cluster populations are stable for several hours.

For an additional test, we use the similarity between the clusters and stable droplets of dense liquid which exist below the liquid-liquid coexistence line in the phase diagram in Fig. 6. The rate of nucleation of the dense droplets was determined by monitoring the increase in time of the number of droplets appearing in an isothermal solution supersaturated with respect to the formation of dense liquid [60]. These data yield droplet nucleation rates, which are of order 10^8 cm^{-3} s^{-1}. These rates are about ten orders of magnitude faster than the rates of crystal nucleation and support the conclusion that the nucleation of the dense liquid precursors, stable or unstable, is much faster than the rate of crystal nucleation within these precursors.

The conclusion that the rate of nucleation of crystals within the dense liquid clusters is the rate determining step in the two-step nucleation mechanism supports the applicability of Eq. (5) as the rate law for this process. Another important consequence of this conclusion is related to the applicability of the nucleation theorem to the two-step nucleation mechanism. Since cluster formation is fast, the clusters can be considered in equilibrium with the solution. Then the chemical potential of the protein in the clusters is equal to the chemical potential of the protein in the solution, and $\Delta\mu = \mu_{solute} - \mu_{crystal}$ is the supersaturation to which the crystal nuclei are exposed within the clusters. Since the cluster number is steady, J is the rate of nucleation of crystals inside the clusters. From the latter two conclusions, it follows that applying the nucleation theorem, Eq. (4) with the macroscopically observed nucleation rate and the external supersaturation, is equivalent to applying the nucleation theorem to the nucleation of crystals in the dense liquid. Hence, the size of the nuclei determined using the nucleation theorem refers to the crystalline nuclei within the clusters.

Furthermore, the transition to spinodal regime occurs when the crystalline nuclei reach size one molecule and this transition corresponds to $\Delta G_2^*=0$.

Finally, we can resolve an apparent controversy. From the above estimate of the lowering of the nucleation rate due to the low volume fraction and the high viscosity of the dense liquid, it may appear that the selection of the two-step mechanism violates the principle of fastest increase of entropy, e.g., [83–84]. This principle governs the selection of kinetic pathways towards, in most cases, the mechanism leading to the fastest rate: faster consumption of supersaturation corresponds to faster increase of the total entropy of the universe. This is an incorrectly posed problem: the estimate of the nucleation rate above used the value of the nucleation barrier ΔG^* extracted from the experimental data. As just demonstrated, this barrier is in fact ΔG_2^* from Fig. 3c and Eq. (5), i.e., the barrier for nucleation of crystals inside the clusters. Since the surface free energy at the interface between the crystal and the solution is likely significantly higher than at the interface between the crystal and the dense liquid, the barrier for nucleation of crystals from the solution would be much higher. This would lead to much slower nucleation of crystals directly from the solution than inside the clusters. Thus, the protein crystal nucleation follows the two-step nucleation mechanism because it provides for faster rate of the solution to crystal phase transition and in this way for faster decrease of the free energy of the system, which corresponds to faster increase of the entropy of the universe.

The role of heterogeneous nucleation substrates

Knowing that the nucleation of crystal within the dense liquid clusters is the rate limiting step in the two-step mechanism, we can address a broader related question: Since from a general point of view, the rate of nucleation via the two-step mechanism depends on two pre-exponential factors, J_{01} and J_{02}, and two barriers, ΔG_1^* and ΔG_2^*, which of these four parameters is the most significant. Clearly, the answer should be sought between J_{02} and ΔG_2^*. Since nucleation occurs in the vicinity of the solution-crystal spinodal, ΔG_2^* is very small, and hence, the most important parameter is J_{02}. This is a surprising conclusion, and it sheds light on the role of heterogeneous substrates in nucleation.

Nucleation is often facilitated by heterogeneous centers [46, 85]. The generally accepted mechanism of heterogeneous nucleation is that it follows the kinetic law for homogeneous nucleation but is faster due to lowering of the nucleation free energy barrier [46]. Since we now know that ΔG_2^* is insignificant, we conclude that in contrast to the generally accepted viewpoint heterogeneous nucleation centers assist nucleation not by lowering ΔG_2^*, but by assisting the growth of the ordered clusters through the factor accounted for in the pre-exponential factor J_{02}.

There may be many mechanisms by which a surface may facilitate the growth of the ordered clusters. The most obvious one is that the “right” crystal structure, i.e., the one that minimizes the free energy of the system, is similar to the structure of the surface. Alternatively, the surface structure may stabilize a necessary intermediary *en route* to the “right” crystal structure, similar to the way enzymes stabilize the transition state, and not the final product of the catalyzed reaction [86]. Another possibility is that the surface may catalyze the formation of the intermolecular bonds in the crystal. If the structure of a substrate is similar to the structure of the growing crystal, this is referred to as templating [87–88]. Examples were found for crystallization of proteins on mineral substrates and on ordered lipid layers [89–90]. One may view the acceleration of nucleation of γ-glycine crystals in the bulk of a supersaturated solution by elliptically polarized light, and α-glycine crystals

by linearly polarized light as examples of assisted structuring of the dense liquid by appropriately structured electric field [91].

Other systems for which the two-step nucleation mechanism applies

Above, we analyzed in detail data on the kinetics of nucleation of crystals of the protein lysozyme, which allow a rather confident conclusion about the applicability of the two-step mechanism. The evidence for the applicability of this mechanism to the nucleation of crystals of other proteins is less direct. In Ref. [92], crystals of several intact immunoglobins were found to coexist for extended lengths of time with dense liquid droplets without the droplets generating additional crystal nuclei. The crystals that were nucleated on the droplet boundaries grew into the dilute solution, rather than into the dense liquid. This was interpreted in favor of nucleation of the crystals within dense liquid clusters suspended in the solution.

Besides the nucleation of protein crystals, the action of the two-step mechanism has recently been demonstrated for the homogeneous nucleation of HbS polymers, with metastable dense liquid clusters serving as precursor to ordered nuclei of the HbS polymer [66, 93–94]. Other studies have shown that the nucleation of amyloid fibrils of several proteins and peptide fragments, such as Alzheimer-causing A-β-peptide or the yeast prion protein follows a variant of the two-step mechanism in which the role of the intermediate liquid state is played by a molten globule of consisting of unfolded protein chains [95–96].

The applicability of the two-step mechanism to the nucleation of crystals of urea and glycine was deduced in a series of experiments, in which high power laser pulses were shone on supersaturated solutions [91, 97]. It was fond that the nucleation rate increases as a result of the illumination by eight-nine orders of magnitude and that by using elliptically or linearly polarized light, α– or γ– glycine crystals could be preferentially nucleated. Since glycine does not absorb the illumination wavelength, and the electric field intensity was insufficient to orient single glycine molecules, it was concluded that the elliptically or linearly polarized pulses stabilize the structure fluctuations within the dense liquid, which lead to the respective solid phases [32, 97].

Colloid systems are the ones for which the evidence in favor of the applicability of the two-step mechanism is the strongest. By tracking the motions of individual particles of size a few microns by scanning confocal microscopy, the nucleation of crystals in colloidal solutions was directly observed [98–100]. These experiments revealed that the formation of crystalline nuclei occurs within dense disordered and fluid regions of the solution [101].

The role of an amorphous precursor in the nucleation of crystal of biominerals has been speculated for a long time, for a historic overview, see 102. However, it was envisioned that the precursor does not facilitate that formation of the crystalline nuclei, but only serves as a source of material for re-precipitation into a crystalline phase. Only recently it was shown that amorphous or liquid clusters of calcium and carbonate ions are present in calcium carbonate solutions and facilitate the nucleation of calcite crystals, in a manner similar to the role of the mesoscopic clusters in lysozyme crystallization discussed above [102–104]. The free energy landscape along the nucleation reaction pathway in Fig. 2c was used to characterize kinetics of the process of calcite crystallization [104].

A two-step nucleation mechanism going through metastable clusters (in this case, swollen micelles) has also been theoretically predicted for a ternary system of two homopolymers and their block-copolymer [105].

Stable dense liquid was found to exist in solutions of organic materials and serve as location where crystals nucleate and grow [26]. The existence of the dense liquid in these solutions has been attributed to the same fundamental physical mechanism as the one acting in protein solutions: the size of the solute molecules is larger than the characteristic lengthscale of the intermolecular interactions in the solution [31]. On the other hand, unpublished evidence from the pharmaceutical industry suggests that in many other cases the stable dense liquid, referred to as "oil" by the practitioners in the field, is so viscous that no crystals can form in it. This is in contrast to the observations in Fig. 7, in which crystals form in the relatively non-viscous dense protein liquid. While this has not been tested, it is possible that the two-step mechanism operates in these organic systems by utilizing dense liquid clusters, similar to those seen in protein, colloid, and calcium carbonate solutions.

The broad variety of systems in which the two-step mechanism operates suggests that its selection by the crystallizing systems in preference to the nucleation of ordered phases directly from the low-concentration solution may be based on general physical principles. This idea is supported by two examples of physical theory: by Sear [106] and by Lutsko and Nicolis [107]. Of particular interest is the latter work. It treated a range of points in the phase diagram of two different model systems which likely encompass a broad variety of real solutions and demonstrated that the two-step formation of crystalline nuclei, via a dense liquid intermediate, encounters a significantly lower barrier than the direct formation of an ordered nucleus and should be faster. Interestingly, the intermediate state resulting from the theory was not stabilized and represents a just a well developed density fluctuation.

Conclusions and perspectives

In this review of the recent advances in the understanding of nucleation of crystals in solutions, we show that the classical nucleation theory fails to provide understanding of several features of measured kinetic curves: nucleation rates, which are orders of magnitude lower than the classical prediction; nucleation kinetics curves which exhibit saturation, or, even more puzzling, maxima and decreasing branches, with increasing supersaturation, as well as the role of the other, stable and unstable, phases possible in solution.

We show that these features of the nucleation kinetics reflect the action of two factors, which are unaccounted by the classical nucleation theory: the existence of a spinodal for the solution to crystal phase transition, and the action of a two-step nucleation mechanism. As the spinodal is reached upon supersaturation increase, the barrier for nucleation of crystals vanishes and further increases in supersaturation do not yield faster nucleation rate. According to the two-step mechanism, the nucleation of crystal, step two, occurs within mesoscopic clusters of dense liquid, step one. While the initial thought provoking results on the nucleation kinetics were obtained for the nucleation of protein crystals, and, correspondingly, the two-step mechanism was first proposed for these types of crystals only, further investigations have shown the validity of this mechanism to several organic, inorganic and colloid materials, including the important class of biominerals.

In general, the two possible intermediate states for the two-step mechanism, the stable dense liquid and the metastable clusters, have distinct mechanisms: the discrepancy of the lengthscale of the intermolecular interactions in the solution and the size of the crystallizing molecules for the stable dense liquid, and the existence of limited lifetime complexes for the clusters. Thus, for a given system the availability of any of these two intermediate states is independent of the other; both of them depend on the exact physicochemical characteristics of the system.

To assess the applicability of the two-step mechanism to the overwhelming majority of untested systems, we note that its action relies of the availability of disordered liquid or amorphous metastable clusters in the homogeneous solutions prior to nucleation. While such clusters have been demonstrated for several protein systems and for calcium carbonate solutions it is likely that not all solutions would support the existence of such clusters with properties allowing the nucleation of crystals in them. In such systems the action of the direct nucleation mechanism might be the only option. On the other hand, an intriguing hypothesis is presented by one of the theories discussed above: that a stabilized intermediate state, as a stable dense liquid, as seen in Fig. 7, or as a metastable mesoscopic cluster, as in Fig. 8, is not needed and the two-step mechanism will act even if the intermediate step is just a density fluctuation. Thus, the two-step mechanism may in fact operate in systems where no intermediate is independently found.

The applicability of the concept of the solution-crystal spinodal appears more straightforward: the nucleation of numerous crystals in industrial and laboratory practice is carried out at such high supersaturations that the nucleation occurs either in the spinodal regime or in the immediate vicinity of this regime, where the nucleus consist of just a few molecules.

Acknowledgments

The ideas discussed in this perspective paper have crystallized over the years in engaging discussions with many colleagues. An incomplete list includes A. Myerson, B. Garetz, D. Oxtoby, Z.-G. Wang, D. Weitz, E. Vlieg, J. DeYoreo, D. Kashchiev, A. Kolomeisky, V Lubchenko, and many others. While their contributions are reflected above, the responsibility for all omissions of facts and slips of logic is entirely mine. Our work on the nucleation of crystals and the physical chemistry of protein solutions has been funded by NHLBI-NIH, NSF, the Petroleum Research Fund of ACS, NASA, and The Welch Foundation. I thank NSF (Grant MCB 0843726) and The Normal Heckerman Advanced Research Program (Grant 003652-0078-2009) for financial support for the work on the paper.

References

1. De Yoreo JJ, Burnham AK, Whitman PK. Developing KH_2PO_4 and KD_2PO_4 crystals for the world's most power laser. International Materials Reviews 2002;47(3):113–152.
2. Reichert P, McNemar C, Nagabhushan N, Nagabhushan TL, Tindal S, Hruza A. Metal-interferon-alpha crystals. 1995;5:441. 734.
3. Brange, J. Galenics of Insulin. Berlin: Springer; 1987. ed.
4. Long ML, Bishop JB, Nagabhushan TL, Reichert P, Smith GD, DeLucas LJ. Protein crystal growth in microgravity review of large scale temperature induction method. J. Crystal Growth 1996;168:233–243.
5. Matsuda S, Senda T, Itoh S, Kawano G, Mizuno H, Mitsui Y. New crystal form of recombinant murine interferon-β. J. Biol. Chem 1989;264:13381–13382. [PubMed: 2668265]
6. Peseta, S.; Langer, JA.; Zoon, KC.; Samuel, CE. Interferons and their actions. In: Richardson, CC.; Boyer, PD.; Dawid, IB.; Meister, A., editors. Annual Review of Biochemistry. Vol. Vol. 56. Palo Alto: Annual Reviews; 1989. p. 727-778.
7. Charache S, Conley CL, Waugh DF, Ugoretz RJ, Spurrell JR. Pathogenesis of hemolytic anemia in homozygous hemoglobin C disease. J Clin Invest 1967;46(11):1795–1811. [PubMed: 6061750]
8. Hirsch RE, Raventos-Suarez C, Olson JA, Nagel RL. Ligand state of intraerythrocytic circulating HbC crystals in homozygote CC patients. Blood 1985;66(4):775–777. [PubMed: 2412615]
9. Eaton, WA.; Hofrichter, J. Sickle cell hemoglobin polymerization. In: Anfinsen, CB.; Edsal, JT.; Richards, FM.; Eisenberg, DS., editors. Advances in protein chemistry. Vol. Vol. 40. San Diego: Academic Press; 1990. p. 63-279.
10. Vekilov P. Sickle-cell haemoglobin polymerisation: is it the primary pathogenic event of sickle-cell anaemia? Brit. J. Haematol 2007;139(2):173–184. [PubMed: 17897293]

11. Berland CR, Thurston GM, Kondo M, Broide ML, Pande J, Ogun O, Benedek GB. Solid-liquid phase boundaries of lens protein solutions. Proc. Natl. Acad. Sci. USA 1992;89:1214–1218. [PubMed: 1741375]
12. Asherie N, Pande J, Pande A, Zarutskie JA, Lomakin J, Lomakin A, Ogun O, Stern LJ, King J, Benedek GB. Enhanced crystallization of the Cys18 to Ser mutant of bovine gammaB crystallin. J Mol Biol 2001;314(4):663–669. [PubMed: 11733987]
13. Dodson G, Steiner D. The role of assembly in insulin's biosynthesis. Current Opinion in Structural Biology 1998;8(2):189–194. [PubMed: 9631292]
14. McPherson, A. Introduction to Macromolecular Crystallography. New Jersey: John Wiley: Hoboken; 2009. ed.
15. Berman HM, Westbrook J, Feng Z, Gilliland G, Bhat TN, Weissig H, Shindyalov IN, Bourne PE. The Protein Data Bank. Nucl. Acids Res 2000;28(1):235–242. [PubMed: 10592235]
16. Gibbs JW. On the equilibrium of heterogeneous substances. Trans. Connect. Acad. Sci 1876;3:108–248.
17. Gibbs JW. On the equilibrium of heterogeneous substances. Trans. Connect. Acad. Sci 1878;16:343–524.
18. Kashchiev, D. Nucleation. Basic theory with applications. Heinemann: Oxford: Butterworth; 2000. ed.
19. Volmer, M. Kinetik der Phasenbildung. Dresden: Steinkopff; 1939. ed.
20. Mutaftschiev, B. Nucleation theory. In: Hurle, DTJ., editor. Handbook of crystal growth. Vol. Vol. I. Amsterdam: Elsevier; 1993. p. 189-247.
21. Vekilov PG, Monaco LA, Thomas BR, Stojanoff V, Rosenberger F. Repartitioning of NaCl and protein impurities in lysozyme crystallization. Acta Crystallogr. Section D 1996;52:785–798. [PubMed: 15299643]
22. Lothe J, Pound GM. On the Statistical Mechanics of Nucleation Theory. The Journal of Chemical Physics 1966;45(2):630–634.
23. Broide ML, Berland CR, Pande J, Ogun OO, Benedek GB. Binary liquid phase separation of lens proteins solutions. Proc. Natl. Acad. Sci. USA 1991;88:5660–5664. [PubMed: 2062844]
24. Muschol M, Rosenberger F. Liquid-liquid phase separation in supersaturated lysozyme solutions and associated precipitate formation/crystallization. J. Chem. Phys 1997;107(6):1953–1962.
25. Petsev DN, Wu X, Galkin O, Vekilov PG. Thermodynamic functions of concentrated protein solutions from phase equilibria. J. Phys. Chem. B 2003;107:3921–3926.
26. Bonnett PE, Carpenter KJ, Dawson S, Davey RJ. Solution crystallization via a submerged liquid-liquid phase boundary: oiling out. Chem. Commun 2003:698–699.
27. ten Wolde PR, Frenkel D. Enhancement of protein crystal nucleation by critical density fluctuations. Science 1997;277:1975–1978. [PubMed: 9302288]
28. Talanquer V, Oxtoby DW. Crystal nucleation in the presence of a metastable critical point. J. Chem. Phys 1998;109(1):223–227.
29. Soga KG, Melrose JM, Ball RC. Metastable states and the kinetics of colloid phase separation. J. Chem. Phys 1999;110(4):2280–2288.
30. Thomson JA, Schurtenberger P, Thurston GM, Benedek GB. Binary liquid phase separation and critical phenomena in a protein water solution. Proc. Natl. Acad. Sci. USA 1987;84:7079–7083. [PubMed: 3478681]
31. Asherie N, Lomakin A, Benedek GB. Phase diagram of colloidal solutions. Phys. Rev. Lett 1996;77(23):4832–4835. [PubMed: 10062642]
32. Oxtoby DW. Crystals in a flash. Nature 2002;420:277–278. [PubMed: 12447425]
33. Vekilov PG. Dense liquid precursor for the nucleation of ordered solid phases from solution. Crystal Growth and Design 2004;4:671–685.
34. Galkin O, Vekilov PG. Control of protein crystal nucleation around the metastable liquid-liquid phase boundary. Proc. Natl. Acad. Sci. USA 2000;97(12):6277–6281. [PubMed: 10823898]
35. Anderson VJ, Lekkerkerker HNW. Insights into phase transition kinetics from colloid science. Nature 2002;416:811–815. [PubMed: 11976674]

36. Galkin O, Vekilov PG. Direct determination of the nucleation rate of protein crystals. J. Phys. Chem 1999;103:10965–10971.
37. Vekilov PG, Galkin O. On the methods of determination of homogeneous nucleation rates of protein crystals. Colloids and Surfaces A 2003;215:125–130.
38. Bhamidi V, Varanasi S, Schall CA. Measurement and modeling of protein crystal nucleation kinetics. Crystal Growth & Design 2002;2(5):395–400.
39. Dixit NM, Kulkarni AM, Zukoski CF. Comparison of experimental estimates and model predictions of protein crystal nucleation rates. Colloids and Surfaces A 2001;190:47–60.
40. Dixit NM, Zukoski CF. Crystal Nucleation Rates for Particles Experiencing Short- Range Attractions: Applications to Proteins. J Colloid Interface Sci 2000;228(2):359–371. [PubMed: 10926476]
41. Kashchiev D. On the relation between nucleation work, nucleus size, and nucleation rate. The Journal of Chemical Physics 1982;76(10):5098–5102.
42. Oxtoby DW, Kashchiev D. A general relation between the nucleation work and the size of the nucleus in multicomponent nucleation. The Journal of Chemical Physics 1994;100(10):7665–7671.
43. Ford IJ. Nucleation theorems, the statistical mechanics of molecular clusters, and a revision of classical nucleation theory. Physical Review E 1997;56(5):5615–5629.
44. Schmeltzer JN. Comments on the nucleation theorem. J. Colloid Interface Sci 2001;242:354–372.
45. van der Waals, JD. Nobel Lectures, Physics 1901–1921. Amsterdam: Elsevier Publishing Company; 1910. The equation of state for gases and liquids.
46. Debenedetti, PG. Metastable Liquids. Princeton: Princeton Univ Pr; 1996. ed.
47. Cahn JW, Hilliard JE. Free energy of a nonuniform system. I. Interfacial free energy. The Journal of Chemical Physics 1958;28(2):258–267.
48. Langer, JS. Spinodal decomposition. In: Riske, T., editor. Fluctuations and Instabilities in Phase Transitions. New York: Plenum; 1975. p. 19-42.
49. Filobelo, L. Kinetics of Phase Transition in Protein Solutions on Microscopic and Mesoscopic Length Scales. Houston: University of Houston; 2005.
50. Pan W, Kolomeisky AB, Vekilov PG. Nucleation of ordered solid phases of protein via a disordered high-density state: Phenomenological approach. J. Chem. Phys 2005;122:174905. [PubMed: 15910067]
51. Vekilov, PG. Incorporation at kinks: kink density and activation barriers. In: Skowronski, M.; DeYoreo, JJ.; Wang, CA., editors. Perspectives on Inorganic, Organic and Biological Crystal Growth: From Fundamentals to Applications: AIP Conference Proceedings; Melville, NY: AIP; 2007. p. 235-267.
52. Van Driessche AES, Otálora Fn, Sazaki G, Sleutel M, Tsukamoto K, Gavira JA. Comparison of Different Experimental Techniques for the Measurement of Crystal Growth Kinetics†. Crystal Growth & Design 2008;8(12):4316–4323.
53. Malkin AJ, Kuznetsov YG, McPherson A. In situ atomic force microscopy studies of surface morphology, growth kinetics, defect structure and dissolution in macromolecular crystallization. J. Crystal Growth 1999;196:471–488.
54. Vekilov PG, Thomas BR, Rosenberger F. Effects of convective solute and impurity transport on protein crystal growth. J. Phys. Chem. B 1998;102:5208–5216.
55. Vekilov PG. What determines the rate of growth of crystals from solution? Crystal Growth and Design 2007;7(12):2796–2810.
56. Petsev DN, Chen K, Gliko O, Vekilov PG. Diffusion-limited kinetics of the solution-solid phase transition of molecular substances. Proc. Natl. Acad. Sci. USA 2003;100:792–796. [PubMed: 12552115]
57. Zel'dovich YB. Theory of new phase formation: Cavitation. Acta Physicochimica URSS 1943;18(11/12):1–22.
58. Kashchiev, D. Nucleation. In: Eerden, JPvd; Bruinsma, OSL., editors. Science and technology of crystal growth. Kluwer Academic Publishers; 1995. p. 53-56.

59. Galkin O, Vekilov PG. Are nucleation kinetics of protein crystals similar to those of liquid droplets? J. Amer. Chem. Soc 2000;122:156–163.
60. Shah M, Galkin O, Vekilov PG. Smooth transition from metastability to instability in phase separating protein solutions. J. Chem. Phys 2004;121:7505–7512. [PubMed: 15473826]
61. Steinrauf LK. Preliminary x-ray data for some crystaline forms of β-lactoglobulin and hen egg-white lysozyme. Acta Crystallogr 1959;12:77–78.
62. Malkin AJ, McPherson A. Light scattering investigations of protein and virus crystal growth: ferritin, apoferritin and satellite tobacco mosaic virus. J. Crystal Growth 1993;128:1232–1235.
63. Malkin AJ, McPherson A. Light scattering investigation of the nucleation processes and kinetics of crystallization in macromolecular systems. Acta Crystallogr. Section D 1994;50(4):385–395. [PubMed: 15299390]
64. Vivares D, Kaler E, Lenhoff A. Quantitative Imaging by Confocal Scanning Fluorescence Microscopy of Protein Crystallization via Liquid-Liquid Phase Separation. Acta Crystallogr D Biol Crystallogr 2005;61:819–825. [PubMed: 15930647]
65. Galkin O, Chen K, Nagel RL, Hirsch RE, Vekilov PG. Liquid-liquid separation in solutions of normal and sickle cell hemoglobin. Proc. Natl. Acad. Sci. USA 2002;99:8479–8483. [PubMed: 12070342]
66. Pan W, Galkin O, Filobelo L, Nagel RL, Vekilov PG. Metastable mesoscopic clusters in solutions of sickle cell hemoglobin. Biophys. J 2007;92(1):267–277. [PubMed: 17040989]
67. Pan W, Vekilov PG, Lubchenko V. The origin of anomalous mesoscopic phases in protein solutions. J. Phys. Chem. B 2010;114:7620–7630. [PubMed: 20423058]
68. Gliko O, Pan W, Katsonis P, Neumaier N, Galkin O, Weinkauf S, Vekilov PG. Metastable liquid clusters in super- and undersaturated protein solutions. J. Phys. Chem. B 2007;111(12):3106–3114. [PubMed: 17388477]
69. Gliko O, Neumaier N, Pan W, Haase I, Fischer M, Bacher A, Weinkauf S, Vekilov PG. A metastable prerequisite for the growth of lumazine synthase crystals. J. Amer. Chem. Soc 2005;127:3433–3438. [PubMed: 15755162]
70. Vekilov, PG.; Pan, W.; Gliko, O.; Katsonis, P.; Galkin, O. Metastable mesoscopic phases in concentrated protein solutions. In: Franzese, G.; Rubi, M., editors. Lecture Notes in Physics, vol. 752: Aspects of Physical Biology: Biological Water, Protein Solutions, Transport and Replication. Heidelberg: Springer; 2008. p. 65-95.
71. Pan W, Filobelo L, Pham NDQ, Galkin O, Uzunova VV, Vekilov PG. Viscoelasticity in Homogeneous Protein Solutions. Physical Review Letters 2009;102(5) 058101.
72. Uzgiris EE, Golibersuch DC. Excess Scattered-Light Intensity Fluctuations from Hemoglobin. Physical Review Letters 1974;32(2):37–40.
73. Sciortino F, Mossa S, Zaccarelli E, Tartaglia P. Equilibrium Cluster Phases and Low-Density Arrested Disordered States: The Role of Short-Range Attraction and Long-Range Repulsion. Phys. Rev. Lett 2004;93 055701.
74. Groenewold J, Kegel WK. Anomalously Large Equilibrium Clusters of Colloids. J. Phys. Chem. B 2001;105(47):11702–11709.
75. Liu Y, Chen W-R, Chen S-H. Cluster formation in two-Yukawa fluids. The Journal of Chemical Physics 2005;122(4) 044507.
76. Mossa S, Sciortino F, Tartaglia P, Zaccarelli E. Ground-State Clusters for Short-Range Attractive and Long-Range Repulsive Potentials. Langmuir 2004;20(24):10756–10763. [PubMed: 15544413]
77. Stradner A, Sedgwick H, Cardinaux F, Poon WCK, Egelhaaf SU, Schurtenberger P. Equilibrium cluster formation in concentrated protein solutions and colloids. Nature 2004;432(7016):492–495. [PubMed: 15565151]
78. Hutchens SB, Wang Z-G. Metastable cluster intermediates in the condensation of charged macromolecule solutions. J. Chem. Phys 2007;127 084912.
79. Kashchiev D. Thermodynamically consistent description of the work to form a nucleus of any size. J. Chem. Phys 2003;118:1837–1851.
80. Fredericks WJ, Hammonds MC, Howard SB, Rosenberger F. Density, thermal expansivity, viscosity and refractive index of lysozyme solutions at crystal growth concentrations. J. Crystal Growth 1994;141:183–192.

81. Filobelo LF, Galkin O, Vekilov PG. Spinodal for the solution-to-crystal phase transformation. J. Chem. Phys 2005;123 014904.
82. Chernov, AA. Modern Crystallography III, Crystal Growth. Berlin: Springer; 1984. ed.
83. Lauffer MA. Entropy -driven Processes in Biology. Molecular Biological Biophysics 1975;20:1–264.
84. Hill A. Entropy production as the selection rule between different growth morphologies. Nature 1990;348(6300):426–428.
85. Walton, AG. Nucleation in liquids and solutions. In: Zettlemoyer, AC., editor. Nucleation. New York: Marcel Dekker; 1969. p. 225-307.
86. Fersht, A. Structure and mechanism in protein science. New York: W.H. Freeman; 1999. ed.
87. Hollingsworth MD. Crystal Engineering: from Structure to Function. Science 2002;295:2410–2413. [PubMed: 11923527]
88. Lee JS, Lee Y-J, Tae EL, Park YS, Yoon KB. Synthesis of Zeolite As Ordered Multicrystal Arrays. Science 2003;301(5634):818–821. [PubMed: 12907797]
89. McPherson A, Shlichta P. The use of heterogeneous and epitaxial nucleants to promote the growt of protein crystals. J. Crystal Growth 1988;90:47–50.
90. Hemming SA, Bochkarev A, Darst SA, Kornberg RD, Ala P, Yang DS, Edwards AM. The mechanism of protein crystal growth from lipid layers. J. Mol. Biol 1995;246(2):308–316. [PubMed: 7869382]
91. Garetz B, Matic J, Myerson A. Polarization switching of crystal structure in the nonphotochemical light-induced nucleation of supersaturated aqueous glycine solutions. Phys. Rev. Lett 2002;89 175501.
92. Kuznetsov YG, Malkin AJ, McPherson A. The liquid protein phase in crystallization: a case study intact immunoglobins. J. Crystal Growth 2001;232:30–39.
93. Galkin O, Nagel RL, Vekilov PG. The kinetics of nucleation and growth of sickle cell hemoglobin fibers. J. Mol. Biol 2007;365(2):425–439. [PubMed: 17069853]
94. Galkin O, Pan W, Filobelo L, Hirsch RE, Nagel RL, Vekilov PG. Two-step mechanism of homogeneous nucleation of sickle cell hemoglobin polymers. Biophys. J 2007;93:902–913. [PubMed: 17449671]
95. Lomakin A, Chung DS, Benedek GB, Kirschner DA, Teplow DB. On the nucleation and growth of amyloid b-protein fibrils: deterction of nuclei and quatification of rate constants. Proc. Natl. Acad. Sci. USA 1996;93:1125–1129. [PubMed: 8577726]
96. Krishnan R, Lindquist SL. Structural insights into a yeast prion illuminate nucleation and strain diversity. Nature 2005;435(7043):765–772. [PubMed: 15944694]
97. Aber JE, Arnold S, Garetz BA. Strong dc Electric Field Applied to Supersaturated Aqueous Glycine Solution Induces Nucleation of the Polymorph. Phys. Rev. Lett 2005;94 145503.
98. Leunissen ME, Christova CG, Hynninen A-P, Royall CP, Campbell AI, Imhof A, Dijkstra M, van Roij R, van Blaaderen A. Ionic colloidal crystals of oppositely charged particles. Nature 2005;437(7056):235–240. [PubMed: 16148929]
99. Savage JR, Dinsmore AD. Experimental Evidence for Two-Step Nucleation in Colloidal Crystallization. Physical Review Letters 2009;102(19) 198302.
100. Zhang TH, Liu XY. Multistep crystal nucleation: A kinetic study based on colloidal crystallization. Journal of Physical Chemistry B 2007;111(50):14001–14005.
101. Kawasaki T, Tanaka H. Formation of a crystal nucleus from liquid. Proceedings of the National Academy of Sciences 2010;107(32):14036–14041.
102. Gower LB. Biomimetic Model Systems for Investigating the Amorphous Precursor Pathway and Its Role in Biomineralization. Chemical Reviews 2008;108(11):4551–4627. [PubMed: 19006398]
103. Pouget EM, Bomans PHH, Goos J, Frederik PM, de With G, Sommerdijk N. The Initial Stages of Template-Controlled CaCO3 Formation Revealed by Cryo-TEM. Science 2009;323(5920):1455–1458. [PubMed: 19286549]
104. Gebauer D, Volkel A, Colfen H. Stable Prenucleation Calcium Carbonate Clusters. Science 2008;322(5909):1819–1822. [PubMed: 19095936]

105. Wang JF, Muller M, Wang ZG. Nucleation in A/B/AB blends: Interplay between microphase assembly and macrophase separation. Journal of Chemical Physics 2009;130(15)

106. Sear RP. Nucleation via an unstable intermediate phase. The Journal of Chemical Physics 2009;131(7) 074702.

107. Lutsko JF, Nicolis G. Theoretical evidence for a dense fluid precursor to crystallization. Phys. Rev. Lett 2006;96 046102.

108. Cacioppo E, Pusey ML. The solubility of the tetragonal form of hen egg white lysozyme from pH 4.0 to 5.4. Journal of Crystal Growth 1991;114:286–292.

109. Howard SB, Twigg PJ, Baird JK, Meehan EJ. The solubility of hen-egg-white lysozyme. J. Crystal Growth 1988;90:94–104.

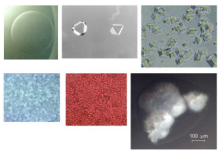

Figure 1.
Nucleation largely determines the outcome of crystallization. Examples of protein crystals and other condensed phases illustrate, at top left, the failure of nucleation, where no crystals or other condensed phase is generated in a supersaturated lysozyme solution; and clockwise from there, the nucleation of two crystals of apoferritin, which grow to a relatively large size; the nucleation of numerous crystals of insulin, which have a broad size distribution; needle-like crystals of lysozyme; dense liquid droplets in a solution of hemoglobin A, and, at bottom left, amorphous precipitate in a supersaturated lysozyme solution. Scale bar is shown in bottom right panel.

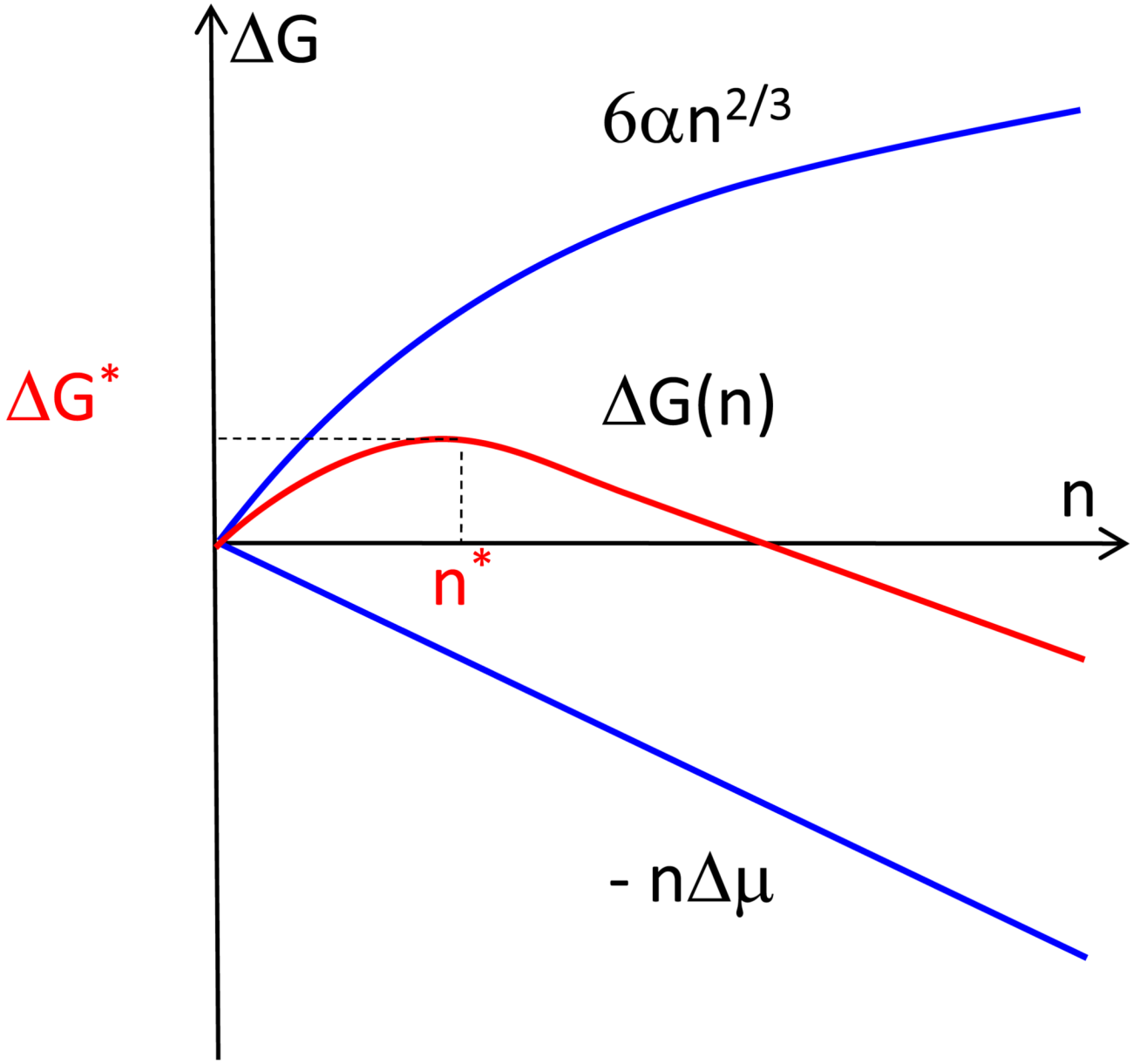

Figure 2.
Illustration of the thermodynamic effects of formation of a crystal. *n* – number of molecules in crystalline embryo; Δμ – solution supersaturation; α – surface free energy; Δ*G* – free energy; * denotes critical cluster.

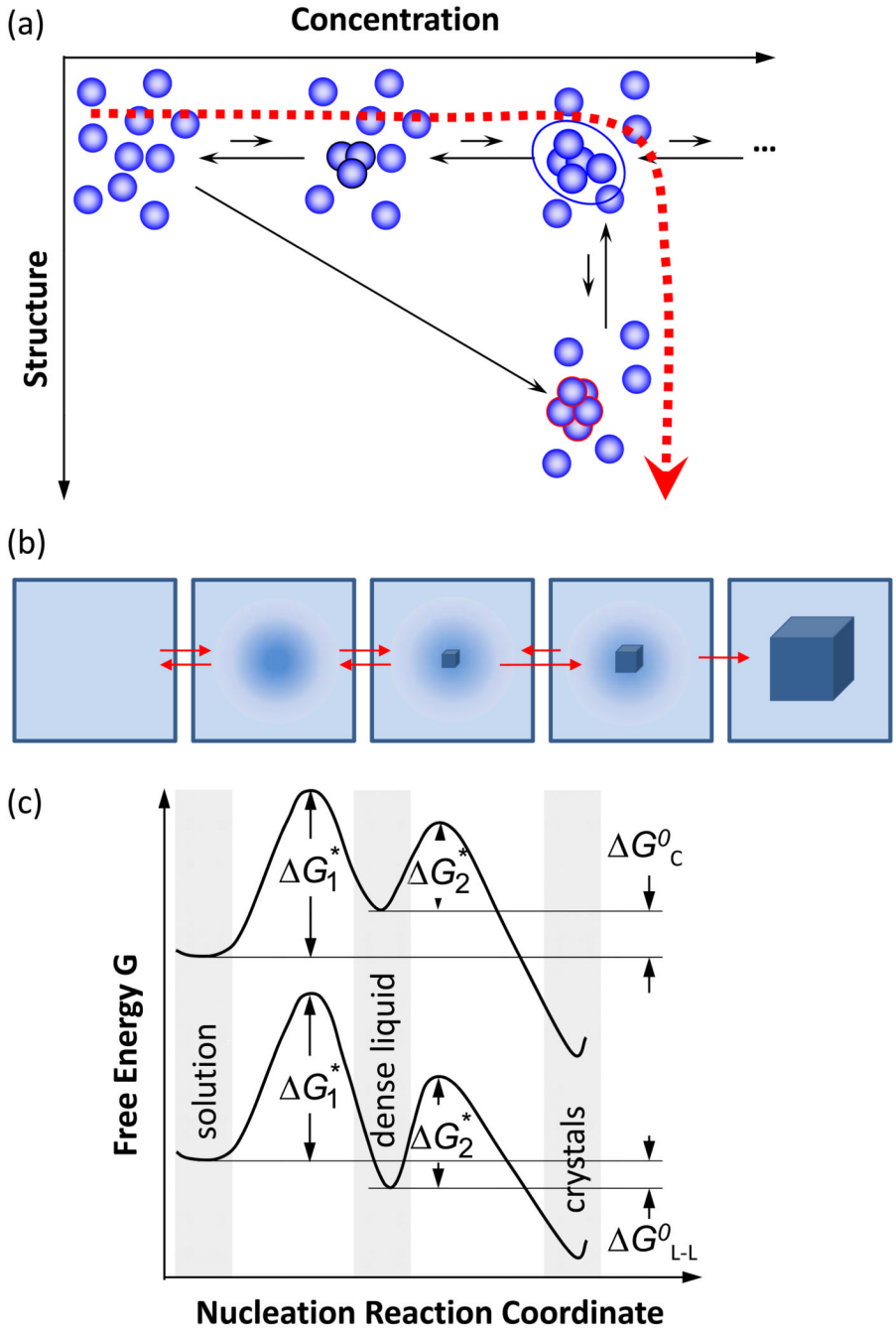

Figure 3.

Schematic illustration of the two-step mechanism of nucleation of crystals. A dense liquid cluster forms. A crystal nucleus may form inside the cluster. (a) Microscopic viewpoint in the (Concentration, Structure) plane; (b) Macroscopic viewpoint of events along thick dashed line in (a). (c) The free-energy ΔG along two possible versions of the two step nucleation mechanism. If dense liquid is unstable and $\Delta G^0_{L\text{–}L}>0$ ($\Delta G^0_{L\text{–}L}$—standard free energy of formation of dense liquid phase), dense liquid exists as mesoscopic clusters, $\Delta G^0_{L\text{–}L}$ transforms to ΔG^0_C, and upper curve applies; if dense liquid is stable, $\Delta G^0_{L\text{–}L}<0$, reflected by

lower curve. ΔG_1^* is the barrier for formation of a cluster of dense liquid, ΔG_2^* – for a formation of a crystalline nucleus inside the dense liquid.

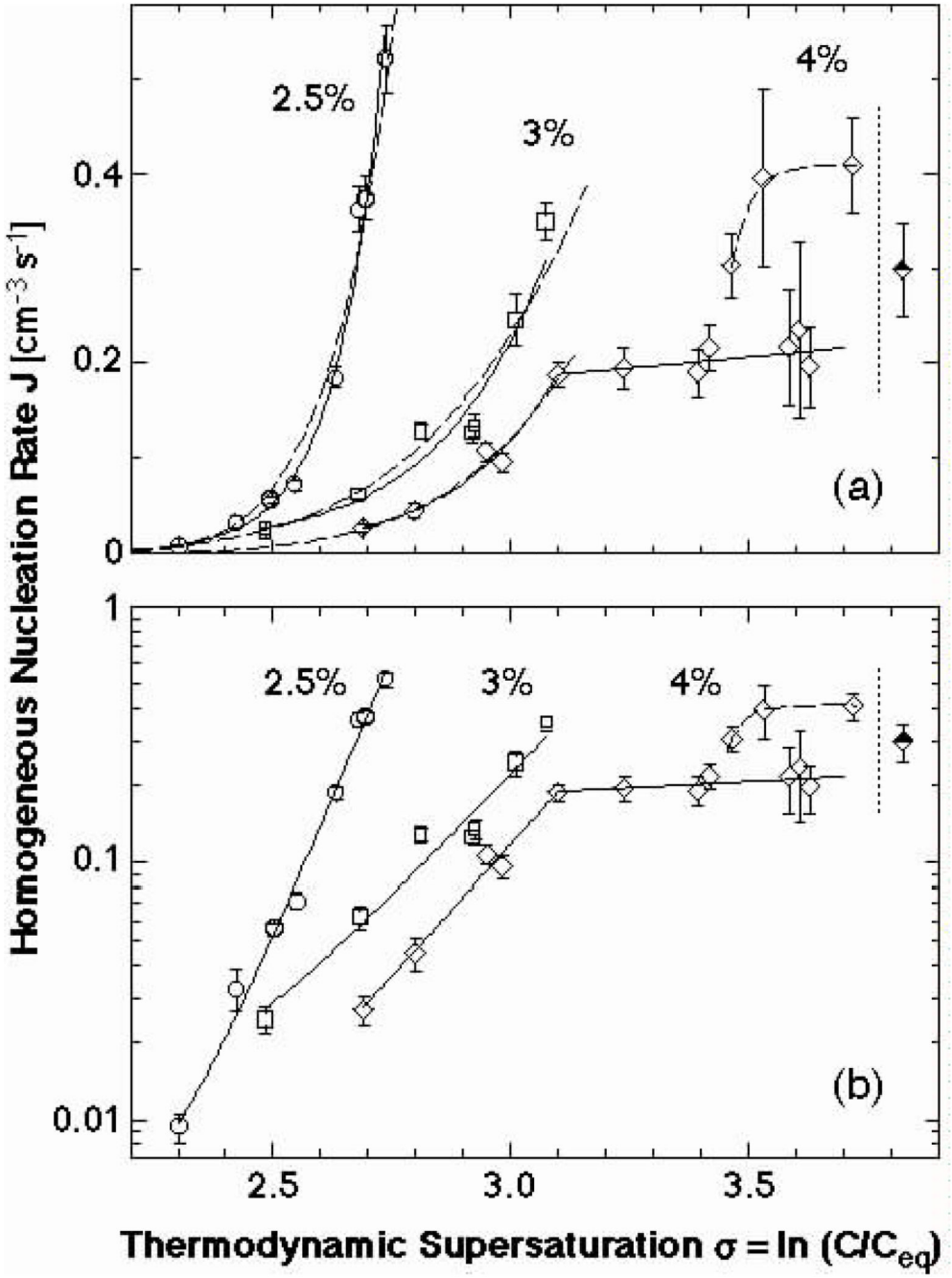

Figure 4.

The dependence of the rate of homogeneous nucleation J of lysozyme crystals of supersaturation $\sigma \equiv \Delta\mu/k_BT$ at T = 12.6 °C and at the three concentrations of the precipitant NaCl indicated on the plots. Solid lines – fits with exponential functions; dashed lines fits with the classical nucleation theory expression, Eq. (3). Vertical dotted lines at σ = 3.9 indicate the liquid-liquid coexistence boundary at this T and C_{NaCl} = 4 %; this supersaturation corresponds to lysozyme concentration 67 mg ml^{-1}. (a) Linear coordinates; (b) semi-logarithmic coordinates. With permission from Ref. [59].

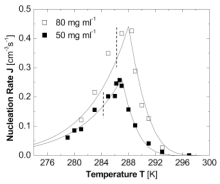

Figure 5.

The dependence of the rate of homogeneous nucleation J of lysozyme crystals on temperature T at two fixed lysozyme concentrations indicated in the plot. The temperatures of equilibrium between crystals and solution are 315 K at C_{lys} = 50 mg ml^{-1} and 319 K at C_{lys} = 80 mg ml^{-1}. The temperatures of L-L separation are 285 K at C_{lys} = 50 mg ml^{-1} and 287 K at C_{lys} = 80 mg ml^{-1} [25] and are marked with vertical dashed lines. Symbols represent experimental results from [34]. Lines are results of two-step model in Eqs. (5)–(7). With permission from Ref. [50].

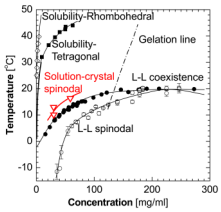

Figure 6.

The phase diagram of a lysozyme solution determined experimentally in 0.05 M Na acetate buffer at pH = 4.5 and 4.0 % NaCl. Liquidus, or solubility lines—from Refs. 108–109, liquid-liquid (L-L) coexistence and respective spinodal—from Ref. 25, gelation line—from Refs. 24–25. Solution-crystal spinodal is highlighted in red and is from Ref. 81.

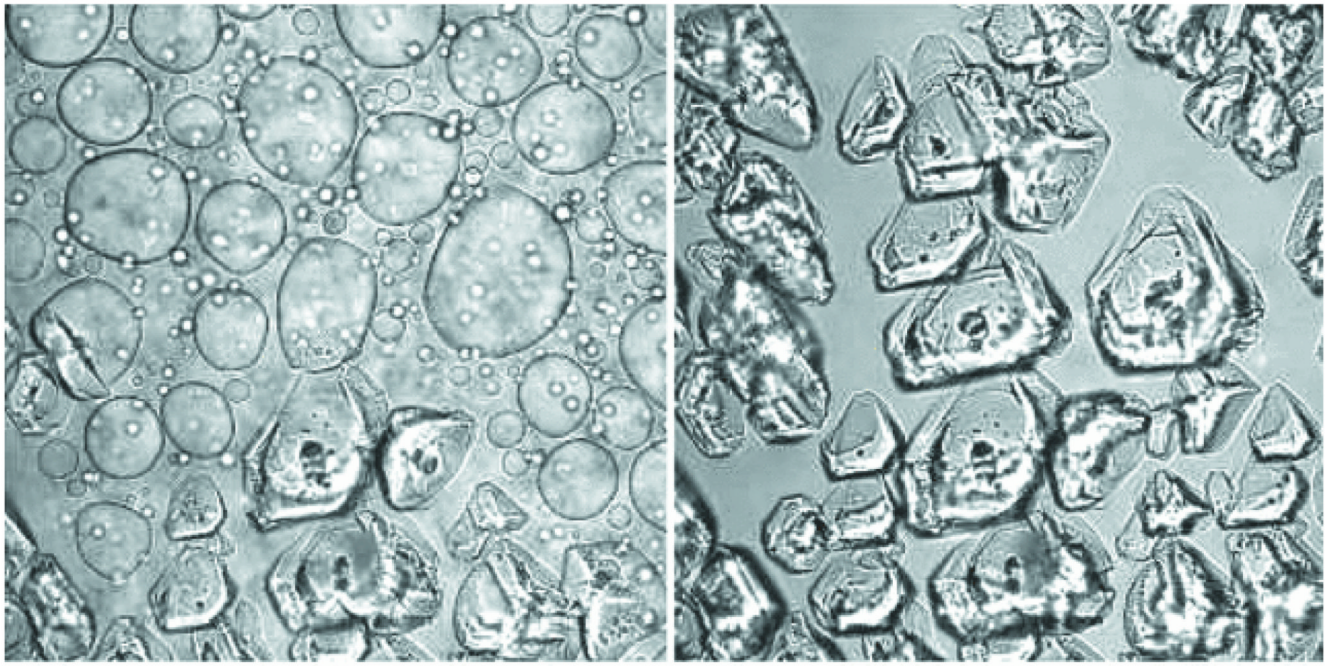

Figure 7.
Confocal scanning laser fluorescence microscopy imaging of nucleation of crystals of glucose isomerase within dense liquid droplets. Bright field imaging, polyethylene glycol with molecules mass 10,000 g mol^{-1} (PEG 10000) used to induce crystallization. The time interval between the left and right images is 380 s. $C_{protein}$ = 55 mg ml^{-1}, C_{PEG} = 9.5%, 0.5 M NaCl, 10 mM Tris maintaining pH = 7. The width of each image is 326 μm. With permission from Ref. [64].

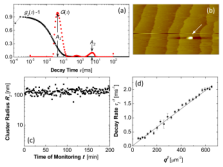

Figure 8.
Characterization of dense liquid clusters. (a) Examples of correlation function of the scattered intensity $g_2(\tau)$ and the respective intensity distribution function $G(\tau)$ of a lysozyme solution with C = 148 mg ml^{-1} in 20 mM HEPES buffer; data collected at angle 145°. (b) Atomic force microscopy imaging of liquid cluster landing on the surface of a crystal in a lumazine synthase solution. Tapping mode AFM imaging, scan width 20 μm. Apparent lateral cluster dimensions are misleading, cluster height is 120 nm, with permission from Ref. [69]. (c) Time dependence of the radius of dense liquid clusters in the same lysozyme solution as in a. (d) The dependence of the decay rate $\Gamma_2 = \tau_2^{-1}$ of the cluster peak in the correlation function on the squared wave vector q^2 for a lysozyme solution as in (a).